

RESEARCH PAPER

Similar hydraulic efficiency and safety across vesselless angiosperms and vessel-bearing species with scalariform perforation plates

Santiago Trueba^{1,2,*}, Sylvain Delzon³, Sandrine Isnard² and Frederic Lens⁴

¹ Department of Ecology and Evolutionary Biology, University of California, Los Angeles, 621 Charles E. Young Dr. South, Los Angeles, CA 90095, USA

² AMAP, IRD, CIRAD, CNRS, INRA, Université de Montpellier, Nouméa, New Caledonia

³ BIOGECO, INRA, Université de Bordeaux, Pessac 33610, France

⁴ Naturalis Biodiversity Center, Leiden University, PO Box 9517, 2300RA Leiden, The Netherlands

* Correspondence: strueba@gmail.com

Received 28 September 2018; Editorial decision 14 March 2019; Accepted 14 March 2019

Editor: Tim Brodribb, University of Tasmania, Australia

Abstract

The evolution of xylem vessels from tracheids is put forward as a key innovation that boosted hydraulic conductivity and photosynthetic capacities in angiosperms. Yet, the role of xylem anatomy and interconduit pits in hydraulic performance across vesselless and vessel-bearing angiosperms is incompletely known, and there is a lack of functional comparisons of ultrastructural pits between species with different conduit types. We assessed xylem hydraulic conductivity and vulnerability to drought-induced embolism in 12 rain forest species from New Caledonia, including five vesselless species, and seven vessel-bearing species with scalariform perforation plates. We measured xylem conduit traits, along with ultrastructural features of the interconduit pits, to assess the relationships between conduit traits and hydraulic efficiency and safety. In spite of major differences in conduit diameter, conduit density, and the presence/absence of perforation plates, the species studied showed similar hydraulic conductivity and vulnerability to drought-induced embolism, indicating functional similarity between both types of conduits. Interconduit pit membrane thickness (T_m) was the only measured anatomical feature that showed a relationship to significant vulnerability to embolism. Our results suggest that the incidence of drought in rain forest ecosystems can have similar effects on species bearing water-conducting cells with different morphologies.

Keywords: Drought resistance, embolism resistance, interconduit pit membrane thickness, New Caledonia, rain forest ecology, scalariform perforation plates, tracheids, vessel elements, vesselless angiosperms, wood anatomy.

Introduction

Along with other relevant functions such as mechanical support and storage of photosynthates, the major function of wood tissue is to transport water from the soil to the transpiring leaves (Badel *et al.*, 2015). Xylem conduits (i.e. tracheary elements) comprise the water-conducting cells enabling long-distance

water transport in vascular plants. Structurally, xylem conduits can be divided into two types: (i) tracheids, which are single-celled water-conducting units with densely pitted lateral walls and without perforations; and (ii) vessels, which are multiple-celled conduits forming long hollow tubes comprised of

single-celled vessel elements that are axially connected by their perforation plates (Sperry, 2003). The evolution of vessels from tracheids has been traditionally considered a major functional transition that happened several times in land plant evolution (Bailey and Tupper, 1918), although intermediate conduit types with various degrees of pit membrane remnants in perforation plates also exist (Carlquist, 1992; Carlquist and Schneider, 2002a). Vessels have enabled plants to develop a more efficient hydraulic pipeline compared with vesselless species, allowing higher leaf vein densities and increased photosynthetic capacities in vessel-bearing species and thereby offering greater competitive advantage over vesselless species (Bailey, 1944; Brodribb and Feild, 2000, 2010; Feild and Wilson, 2012; Feild and Brodribb, 2013).

Vessellessness is a rare feature in angiosperms since it is restricted to only a few clades such as Acorales, Amborellales, Nymphaeales, Trochodendrales, and Winteraceae (Spicer and Groover, 2010; Olson, 2014). Because of their structurally driven low transpiration rates, most vesselless angiosperms and angiosperms with vessel elements having densely barred scalariform perforation plates have probably occupied mesic habitats since their origin (Feild *et al.*, 2003, 2004). For instance, the New Caledonian vesselless shrub *Amborella trichopoda*, which is sister to all other extant angiosperms, is mainly found in the moist understorey of rain forest environments with closed canopies and presents the architectural characteristics of a shade-adapted plant (Feild and Arens, 2007; Trueba *et al.*, 2016). The environmental preferences of vesselless angiosperms suggest a low adaptation to drought stress, which probably has restricted these species to humid environments. Vessel elements with oblique scalariform perforation plates bearing many bars can be considered morphologically as intermediate between tracheids and vessel elements with simple perforation plates (Carlquist and Schneider, 2002a). Despite being derived from a tracheid-based xylem, vessel-bearing species with perforation plates including many closely spaced bars are hypothesized to have a similar, rather inefficient, hydraulic performance compared with vesselless angiosperms due to the high flow resistance exerted by their scalariform perforation plates (Christman and Sperry, 2010; Hudson *et al.*, 2010; Feild *et al.*, 2011). Moreover, it has been shown that pit membrane remnants are usually present in these types of scalariform perforations (Carlquist, 1992; Carlquist and Schneider, 2002a, b), which further impedes hydraulic performance (Feild and Wilson, 2012). Little is known about the xylem anatomical features associated with the hydraulic performance of these species, although a recent study has shown that hydraulic vulnerability is a major driver of rain forest habitat occupation in vesselless and vessel-bearing New Caledonian angiosperms (Trueba *et al.*, 2017).

Anatomical features such as conduit diameter and density have a direct effect on the efficiency and safety of water conductivity (Pittermann and Sperry, 2003; Loepfe *et al.*, 2007; Zanne *et al.*, 2010; Gleason *et al.*, 2016b). For instance, wide conduits reduce resistance to flow, and thus increase hydraulic efficiency (Hacke *et al.*, 2006, 2017). Yet, it has been proposed that vesselless angiosperms do not show a significant increase in flow conductivity with increasing conduit diameter (Hacke *et al.*, 2007). Because hydraulic conductivity efficiency is proportional to the sum of the conduit diameters to the fourth power according to

Poiseuille's law (Tyree and Zimmermann, 2002), it is possible to estimate theoretical hydraulic conductivity using anatomical variables. However, no study to date has carried out a comparison of theoretical and native hydraulic conductivity across vesselless and vessel-bearing angiosperms with scalariform perforation plates. Along with transport efficiency, hydraulic safety is also an important feature that is influenced by wood anatomical features (Lens *et al.*, 2011; Li *et al.*, 2016). Safety in water transport reflects the ability of plants to cope with high xylem tensions within the conduits, which could lead to a partial air-filled blockage of the water transport pathway due to drought-induced embolism formation. In theory, after embolism occurrence, species with wider and less numerous conduits should be more affected because greater conductive surfaces are impacted. In addition to conduit diameter and density, the ratio between the thickness (t) of two adjacent conduit walls and the conduit lumen diameter (b) has been proposed to relate to xylem embolism resistance by providing a mechanical reinforcement of conduit walls acting as a safety factor from potential implosion by negative pressure (Hacke *et al.*, 2001; Jacobsen *et al.*, 2005). As an example, tracheid wall thickness has been shown to be an important functional trait in the earlywood of conifers (Rosner *et al.*, 2018), as well as the thickness-to-diameter ratio in the leaf vasculature (Jordan *et al.*, 2013).

Since both tracheids and vessels are limited in length, and are always much shorter than the size of the entire plant, both tracheids and vessels have bordered interconduit pits in their lateral walls through which water can be laterally transported from one conduit to an adjacent conduit (Sano *et al.*, 2011; Lens *et al.*, 2013). Fine-scale features of these interconduit pits, especially those related to the pit membrane, have been demonstrated to play a major role in avoiding air bubble propagation throughout the 3D conduit network and thereby contributing to embolism resistance in angiosperms, gymnosperms, and pteridophytes (Choat *et al.*, 2008; Delzon *et al.*, 2010; Pittermann *et al.*, 2010; Lens *et al.*, 2011; Brodersen *et al.*, 2014; Schenk *et al.*, 2015; Li *et al.*, 2016). Bordered pit features conferring embolism resistance have been analyzed in conifer tracheids, showing the main role of the overlap between torus and pit aperture (Delzon *et al.*, 2010; Bouche *et al.*, 2014). However, tracheids in vesselless angiosperms have homogeneous pit membranes that are devoid of the torus-margo structure. The thickness of the pit membrane (T_m) has been suggested to be a major determinant of embolism resistance in angiosperm vessels (Lens *et al.*, 2011; Li *et al.*, 2016; Dória *et al.*, 2018). Thicker T_m increases the tortuous path length that air needs to cross before reaching an adjacent water-filled conduit, therefore impeding air-seeding between adjacent conduits, and this mechanism could explain the direct functional link between T_m and embolism resistance (Jansen *et al.*, 2009; Lens *et al.*, 2013; Li *et al.*, 2016). Given that air bubble expansion occurs immediately after air entry through a pit membrane, the most likely space for air bubble expansion is within the limits of the pit borders (Schenk *et al.*, 2015). Accordingly, pit chamber depth (L_p), which is the distance between the roof of the pit border and the position of the relaxed pit membrane, has also been suggested as being related to embolism resistance in angiosperm vessels (Lens *et al.*, 2011).

A recent study analyzed the relationship between the xylem pressure inducing 50% loss of xylem hydraulic conductivity (P_{50}) and the intertracheid pit structure in six vesselless angiosperm species, showing a lack of correlation between P_{50} and T_m (Zhang *et al.*, 2017). Yet, the study of Zhang *et al.* (2017) used P_{50} values collected from the literature, and did not include anatomical measurements from the same individuals for which the hydraulic data were generated. Here, we assess these structure–function correlations using data from the same individuals, and we include vesselless and vessel-bearing species with scalariform perforation plates inhabiting a similar rain forest ecosystem. Moreover, with the exception of *Amborella trichopoda*, we investigate species that have not been included in previous studies.

In this study, we analyze xylem hydraulic efficiency versus safety along with stem anatomical features (Table 1), with a special focus on fine-scale observations of interconduit pits in vesselless and vessel-bearing species native to the New Caledonian rain forests. We aim to test the hypotheses that: (i) vessel-bearing species with scalariform perforation plates show hydraulic conductivity and vulnerability to embolism similar to vesselless species occurring in the same environment; (ii) the diameter, density, and wall structure of xylem conduits are associated with xylem hydraulics, with species which have wider conduits with proportionally thinner walls being hydraulically more efficient but also more vulnerable; and (iii) ultrastructural variation in the thickness of interconduit pits of both vesselless and vessel-bearing species is functionally linked with vulnerability to embolism. Analyzing vesselless and vessel-bearing species with putative ancestral features such as scalariform perforation plates helps our understanding of the early stages of the hydraulic evolution in flowering plants. Finally, we provide meaningful information regarding the mechanisms that confer drought tolerance in a unique tropical island ecosystem that can be threatened by deficits in rainfall regimes.

Materials and methods

Plant material and sampling

Twelve woody species endemic to New Caledonia were studied (Table 2). All studied species are evergreen and have diffuse-porous wood without

growth ring boundaries. Among the studied species, seven are vessel bearing and have vessel elements with long and obliquely oriented scalariform perforation plates (Table 2). Vessel-bearing species belong to the families Atherospermataceae, Chloranthaceae, Monimiaceae, and Paracryphiaceae. The five studied vesselless species belong to the Amborellaceae and the Winteraceae, which are the only families of vesselless angiosperms present in the New Caledonian archipelago. The woody growth forms of the sampled species vary from shrubs such as *Amborella trichopoda* and *Ascarina rubricaulis*, to trees such as *Nemuaron viellardii* and *Hedycarya parvifolia*. All studied species are present in rain forest ecosystems. However, they differ in their percentage of rain forest occupancy (Pouteau *et al.*, 2015). Fifteen terminal and sun-exposed branches per species were collected at pre-dawn from three individuals. Branches were defoliated, wrapped in moist paper towels with ultrapure water, and sealed in dark plastic bags during transport.

Xylem hydraulic conductivity and embolism vulnerability

Hydraulic measurements of sampled branches were carried out in the plant hydraulics phenotyping platform of the BIOGECO laboratory in Pessac, France. Samples were stored at 5 °C before transportation, and measurements were done within 2 weeks after collection. We verified the absence of pathogens before performing measurements. Branches were excised under water to 27 cm segments. Both ends of the branches were debarked and clipped with a fresh razor blade. The embolism vulnerability of branch segments was then measured using the Cavitation technique (Cochard *et al.*, 2005), which uses centrifugal forces to lower the xylem pressure while simultaneously measuring hydraulic conductivity. This allowed us to measure xylem-specific hydraulic conductivity (K_s , in $\text{kg m}^{-1} \text{MPa}^{-1} \text{s}^{-1}$) using the maximum measured conductivity divided by sample length and sapwood area as averaged from both ends of the sample. Percentage losses of hydraulic conductivity for the analyzed species were obtained from a previous study (Trueba *et al.*, 2017). The vulnerability curves included in this study were reassessed fitting the Weibull function proposed by Ogle *et al.* (2009), which was implemented using the R package ‘fitplrc’ (Duursma and Choat, 2017). P_{50} , the xylem pressure inducing a 50% loss of hydraulic conductivity, and S_{50} , the slope of the curve at P_{50} , which relates to the speed of xylem embolism propagation, were calculated from the vulnerability curves built using the Weibull function. In addition to P_{50} , which is the most commonly used index of embolism resistance (Choat *et al.*, 2012), we also extracted P_{12} . P_{12} is the xylem pressure inducing a 12% loss of hydraulic conductivity, which corresponds to the point of air-entry according to Domec and Gartner (2001) and Martin-StPaul *et al.* (2017). Mean water potentials inducing loss of stem hydraulic conductivity and their corresponding slope values were calculated from 6–11 samples per species.

Table 1. Abbreviations and definitions of xylem anatomical and hydraulic variables measured, with reference to their units

Abbreviation	Definition	Units employed
CD	Xylem conduit density per unit sapwood area	$n \text{ mm}^{-2}$
D_H	Hydraulically weighted mean conduit diameter	μm
D_m	Horizontal pit membrane diameter	μm
D_{pa}	Horizontal pit aperture diameter	μm
K_s	Measured stem hydraulic conductivity	$\text{kg m}^{-1} \text{MPa}^{-1} \text{s}^{-1}$
K_{th}	Theoretical xylem specific hydraulic conductivity	$\text{kg m}^{-1} \text{MPa}^{-1} \text{s}^{-1}$
L_p	Depth of pit chamber from relaxed pit membrane to inner edge of pit aperture	nm
P_{12}	Water potential at 12% loss of stem hydraulic conductivity	MPa
P_{50}	Water potential at 50% loss of stem hydraulic conductivity	MPa
S_{50}	Slope of the vulnerability curve at P_{50}	$\% \text{MPa}^{-1}$
T_w	Double thickness of two adjacent conduits	μm
T_m	Thickness of the interconduit pit membrane	nm
$(t/b)^2$	Xylem conduit wall reinforcement	No unit

Table 2. Origin of species studied in New Caledonia, along with the phylogenetic placement at the family level, and the anatomical and hydraulic observations

Species	Family	Locality	Conduit	K_s	K_{th}	P_{12}	P_{50}	S_{50}	CD	D_H	L_p	T_w	T_m	$(t/b)^2$
<i>Amborella trichopoda</i>	Amborellaceae	Mt. Aoupinié	T	0.437	7.74	-2.17	-2.68	105	1229.49	22.53±0.79	919±23	5.39±0.16	273±13	0.09±0.010
<i>Ascarina rubricaulis</i>	Chloranthaceae	Mt. Dzumac	V, Sc	0.890	24.12	-1.59	-2.28	71	237±21	45.17±1.49	1156±41	6.88±0.21	260±13	0.04±0.005
<i>Hedycarya cupulata</i>	Monimiaceae	Mt. Aoupinié	V, Sc	0.104	6.83	-1.39	-3.09	24	173±15	35.64±1.37	988±37	5.41±0.26	348±7	0.05±0.009
<i>Hedycarya parvifolia</i>	Monimiaceae	Mt. Aoupinié	V, Sc	0.233	12.36	-2.39	-3.23	60	148±18	39.03±1.48	1246±90	9.07±0.35	388±26	0.04±0.004
<i>Kibarpopsis caledonica</i>	Monimiaceae	Mt. Aoupinié	V, Sc	0.257	12.08	-1.55	-2.49	50	236±11	38.04±1.02	1005±53	7.43±0.15	268±15	0.05±0.004
<i>Nemuaron viellarzii</i>	Atherospermataceae	Mt. Dzumac	V, Sc	0.791	23.03	-1.43	-2.30	54	307±19	41.85±1.42	915±58	6.96±0.41	202±8	0.06±0.012
<i>Paracaryphia alticola</i>	Paracaryphiaceae	Mt. Humboldt	V, Sc	0.161	2.73	-0.77	-2.02	30	136±10	30.09±0.71	694±42	5.69±0.20	169±8	0.04±0.003
<i>Quintinia major</i>	Paracaryphiaceae	Mt. Humboldt	V, Sc	0.135	6.91	-1.08	-2.47	29	180±9	35.39±0.55	855±73	7.79±0.33	229±9	0.08±0.025
<i>Zygogynum acsmithii</i>	Winteraceae	Wadjana, Yaté	T	0.566	11.53	-2.39	-2.73	162	1211±48	24.98±0.82	1031±20	9.78±0.32	253±6	0.23±0.021
<i>Zygogynum crassifolium</i>	Winteraceae	Pic du Pin, Yaté	T	0.615	3.87	-3.50	-4.11	89	1037±24	19.77±0.50	1259±77	13.25±0.31	274±16	0.55±0.040
<i>Zygogynum stipitatum</i>	Winteraceae	Wadjana, Yaté	T	0.325	5.53	-1.80	-2.44	78	1121±59	21.19±0.74	921±36	9.79±0.26	215±6	0.36±0.042
<i>Zygogynum thieghemii</i>	Winteraceae	Mt. Humboldt	T	0.658	7.62	-1.62	-2.29	75	862±36	24.52±0.79	1289±91	13.59±0.37	276±17	0.46±0.039

Values are means ±SE. The main conductive elements in xylem are indicated as 'T'=tracheids in vesselless species; 'V, Sc'=vessels with scalariform perforation plates in vessel-bearing species. See Table 1 for a description of abbreviations and units of measurements.

Xylem conduit measurements and analyses

Wood cubes of ~10 mm² were sampled from two branches used for the hydraulic measurements. Transverse sections 30–50 µm thick were made using a sliding microtome. After sectioning, sections were treated with sodium hypochlorite and stained with 0.1% toluidine blue aqueous solution for 5–10 min. In parallel, a mixture of safranin and alcian blue (35:65) was also used for tissue staining. Stained sections were suspended in the mounting medium Euparal (Waldeck GmbH & Co, Münster, Germany) and mounted on microscope slides for imaging. Cross-section images were obtained using a light microscope equipped with a digital camera (Leica DM5000B; Leica Microsystems, Wetzlar, Germany). Images were carried out at five random positions on the mounted wood sections. All anatomical measurements on digital images were carried out using ImageJ 1.50v (National Institutes of Health, Bethesda, MD, USA). Measurements were carried out on 25 randomly selected conduits per sample, resulting in 50 xylem conduits measured per species. We measured the inner lumen area of xylem conduits, and conduit diameter was derived from this measurement assuming a circular shape. The hydraulically weighted conduit diameter (D_H), which corresponds to the mean diameter required to achieve equal conductivity with the same number of conductive elements, was calculated according to Tyree and Zimmermann (2002) using the equation:

$$D_H = \left[\frac{\sum D^4}{N} \right]^{0.25}$$

where D is the diameter of an individual conduit and N is the number of conduits measured. Conduit density (CD, $n \text{ mm}^{-2}$) was estimated in four randomly selected 0.25 mm² images per sample. CD was calculated as the outcome of the number of conduits per square millimeter. Both D_H and CD were used to estimate the xylem-specific theoretical hydraulic conductivity (K_{th} , $\text{kg m}^{-1} \text{ MPa}^{-1} \text{ s}^{-1}$) also known as potential conductivity (Fichot et al., 2010; Poorter et al., 2010). In spite of the potential presence of both tracheids and vessels in the xylem of some vessel-bearing species, only the vessels, which were considered as the main water-conducting cells, were considered for K_{th} estimations. K_{th} was calculated based upon the Hagen–Poiseuille law using the equation:

$$K_{th} = \frac{\pi \rho_w}{128 \eta} \times \text{CD} \times D_H^4$$

Where ρ_w is the density of water at 20 °C (998.2 kg m^{-3}) and η is the viscosity of water at 20 °C ($1.002 \times 10^{-9} \text{ MPa s}^{-1}$). Measurements of the double thickness of two adjacent conduits (T_w , µm) were carried out to estimate xylem conduit wall reinforcement enabling conduit implosion resistance (Hacke et al., 2001). The index of safety from implosion by negative pressure was estimated as $(t/b)^2$, where t is the thickness of two adjacent conduit walls and b is the conduit lumen diameter.

Xylem conduit ultrastructure and lateral pit anatomical measurements

We measured ultrastructural traits of interconduit pits using images obtained from TEM. For TEM imaging, wood samples from the fresh branches used for the Cavitrion experiments were cut into ~2 mm³ blocks and fixed in Karnovsky solution containing formaldehyde and glutaraldehyde (Karnovsky, 1965). Samples were then rinsed using a 0.1 M cacodylate buffer and post-fixed with 2% osmium tetroxide for 2 h. Samples were gradually dehydrated using increasing propanol concentrations. Subsequently, samples were embedded using Epon 812n (Electron Microscopy Sciences, Hatfield, UK) and polymerized at 60 °C for 48 h. Embedded samples were sectioned into 2 µm thick transverse sections. Sections were examined to detect areas of contact between conduits (vessel–vessel or tracheid–tracheid). After trimming, these areas were re-cut into 90 nm thick transverse sections using a diamond knife. The sections were coated on copper grids using Formvar coating (Agar Scientific, Stansted, UK). TEM micrographs were made using a JEM 1400-Plus transmission electron microscope (JEOL, Tokyo, Japan). Lateral

pit ultrastructural characteristics were measured following the protocols described by Scholz *et al.* (2013). Given that we discarded images with visually damaged pit membranes or with insufficient contrast, the number of measurements per species varied depending on the amount of quality micrographs. More than 25 observations were made for most species except *H. parvifolia* (17), *Zygogynum crassifolium* (15), and *Zygogynum tieghemii* (19). Pit membrane thickness (T_m , nm) was measured at one point near the center of the pit membrane. Pit chamber depth (L_p , nm) was measured as the distance from the roof of the pit border (close to the aperture) to the relaxed position of the pit membrane. Pit aperture diameter (D_{pa} , μm) and pit membrane diameter (D_m , μm) were also measured in TEM images. TEM imaging was done on fresh material to avoid potential thickness underestimations derived from the desiccation and alteration of pit membrane structural properties (Scholz *et al.*, 2013; Li *et al.*, 2016; Zhang *et al.*, 2017). We also used SEM micrographs to observe qualitative features of xylem conduits and perforation plate morphology in radial segments. SEM micrographs were acquired using a desktop Phenom G2 Pro scanning electron microscope (Phenom-World BV, The Netherlands) with magnifications between $\times 1500$ and $\times 20\,000$, and an acceleration voltage of 5 kV.

Statistical and phylogenetic analyses

Hydraulic and anatomical traits were assembled and averaged for each species for data analysis. For each trait, assumptions of residual homogeneity and normality were tested prior to analysis. We explored relationships between anatomical traits across species using pairwise Pearson's correlation analyses and regression analyses. Linear regression analyses were used to determine the influence of anatomical variables on the hydraulic performance and the species vulnerability to embolism. Given that inferences about the adaptive value of correlations obtained from standard methods can be biased by the potential affinity of closely related species (Felsenstein, 1985), we analyzed trait correlations using phylogenetically independent contrast (PIC) correlations using the R package 'ape' (Paradis *et al.*, 2004). We built a phylogenetic tree using as a backbone the phylogeny of seed plants available in Smith and Brown (2018), which includes a branch length calibration based on Magallón *et al.* (2015). Molecular data were available for nine out of the 12 studied species. We used the package 'ape' to trim the tree and select the species studied. The species included in the tree were *A. trichopoda*, *A. rubricaulis*, *Hedyccarya cupulata*, *H. parvifolia*, *Kibarpopsis caledonica*, *Paracryphia alticola*, *Zygogynum acsmithii*, *Z. crassifolium*, and *Z. tieghemii* (see Supplementary Fig. S1 at JXB online).

To assess the relationship between theoretical and measured hydraulic conductivity, given that this relationship holds between two 'dependent' variables, we fitted a standardized major axis (SMA) regression using the R package 'smatr' (Warton *et al.*, 2012). Additionally, we employed one-way ANOVAs to assess trait variability across species. To explore the effect of lateral pit aperture ultrastructure on embolism resistance, we analyzed a possible joint effect of L_p and T_m , two traits that have been reported as having an important role on embolism resistance (Lens *et al.*, 2011), on embolism resistance thresholds (P_{12} and P_{50}). We performed multiple regression analyses, and the strength of the contribution of each ultrastructural trait to embolism resistance was evaluated using semi-partial correlations. Xylem hydraulic and anatomical traits of vesselless and vessel-bearing angiosperms were compared using independent-samples *t*-tests. All the analyses were considered significant at $P \leq 0.05$. All statistical analyses were performed using R v.3.4.1 (R Core Team, 2017).

Results

Xylem conduit density, diameter, and wall thickness

Vesselless and vessel-bearing species differed significantly in D_H and CD (Fig. 1; Table 3). D_H ranged from 19.77 ± 0.5 μm (mean \pm SE) in the tracheid-bearing *Zygogynum crassifolium*, to 45.17 ± 1.49 μm in the vessel-bearing *Ascarinia rubricaulis*

(Table 2). Average tracheid D_H across vesselless species was 22.60 ± 0.98 μm , and average vessel D_H across vessel-bearing species was 38.45 ± 1.98 μm . CD varied widely across species [$F(11)=199$; $P \leq 0.001$]. CD ranged from 136 ± 10 conduits mm^{-2} to 1229 ± 49 conduits mm^{-2} , measured in *P. alticola* and *A. trichopoda*, respectively. Xylem conduit wall reinforcement, $(t/b)^2$ presented significant variation both across species [$F(11)=66.79$; $P \leq 0.001$] and across conduit types (Table 3). Vesselless species showed significantly higher $(t/b)^2$ than vessel-bearing species (Fig. 2a; Table 3). The highest wall reinforcement was observed in vesselless species such as *Z. tieghemii* and *Z. crassifolium*, with $(t/b)^2$ values of 0.46 ± 0.039 and 0.55 ± 0.040 , respectively. Average T_w of vesselless species was 10.36 ± 1.48 μm , and average T_w of vessel-bearing species was 7.03 ± 0.47 μm . T_w varied widely across species [$F(11)=73.34$; $P \leq 0.001$]. However, there were no significant differences in T_w between vascular types.

Interconduit pit ultrastructure

T_m varied significantly across species [$F(12)=29.94$; $P \leq 0.001$] from a minimum of 169 ± 8 nm in the vessel-bearing *P. alticola* to a maximum of 388 ± 26 nm in the vessel-bearing *H. parvifolia*. Mean T_m in vesselless species was 258 ± 12 nm, which was not significantly different from the mean T_m in vessel-bearing species (266 ± 30 nm; Fig. 2b; Table 3). L_p also varied significantly across species [$F(11)=26.4$; $P \leq 0.001$], from 694 ± 42 nm in *P. alticola* to 1289 ± 91 nm in *Z. tieghemii*. Vesselless species had a mean L_p of 1084 ± 80 nm, similar to the mean L_p in vessel-bearing species (980 ± 70 nm; Table 3). The other two interconduit pit traits measured, D_{pa} and D_m , had significant variation across species [$F(11)=25.97$; $P \leq 0.001$; and $F(11)=9.01$; $P \leq 0.001$; respectively]. D_{pa} varied from 1.42 ± 0.11 μm to 6.83 ± 0.58 μm , measured in *Z. acsmithii* and *A. rubricaulis*, respectively. D_m ranged from 5.76 ± 0.81 μm to 11.71 ± 0.68 μm , measured in *Quintinia major* and *A. rubricaulis*, respectively. Both lateral wall pit traits were not significantly different between vessel-bearing and vesselless species (Table 3).

Hydraulic conductivity and drought-induced vulnerability to embolism

K_{th} varied from 2.73 $\text{kg m}^{-1} \text{MPa}^{-1} \text{s}^{-1}$ in the vessel-bearing *P. alticola*, which is theoretically the least conductive efficient species, to 24.12 $\text{kg m}^{-1} \text{MPa}^{-1} \text{s}^{-1}$ in the vessel-bearing *A. rubricaulis*, which was the most conductive efficient species according to estimations based on anatomical measurements. K_{th} did not significantly differ in species with different vascular types ($P=0.153$): average K_{th} was 7.26 ± 1.29 $\text{kg m}^{-1} \text{MPa}^{-1} \text{s}^{-1}$ in vesselless species and 12.58 ± 3.1 $\text{kg m}^{-1} \text{MPa}^{-1} \text{s}^{-1}$ in vessel-bearing species (Fig. 2c; Table 3). Similarly, measured stem hydraulic conductivity (K_s) did not differ between vesselless and vessel-bearing species ($P=0.300$; Fig. 2d; Table 3). K_s and K_{th} had a significant correlation (Fig. 3). K_s ranged from 0.104 $\text{kg m}^{-1} \text{MPa}^{-1} \text{s}^{-1}$ in *H. cupulata* to 0.890 $\text{kg m}^{-1} \text{MPa}^{-1} \text{s}^{-1}$ in *A. rubricaulis*; both species have vessel-bearing xylem.

Xylem vulnerability to embolism was not significantly different between conduit types: vesselless species had a mean P_{50}

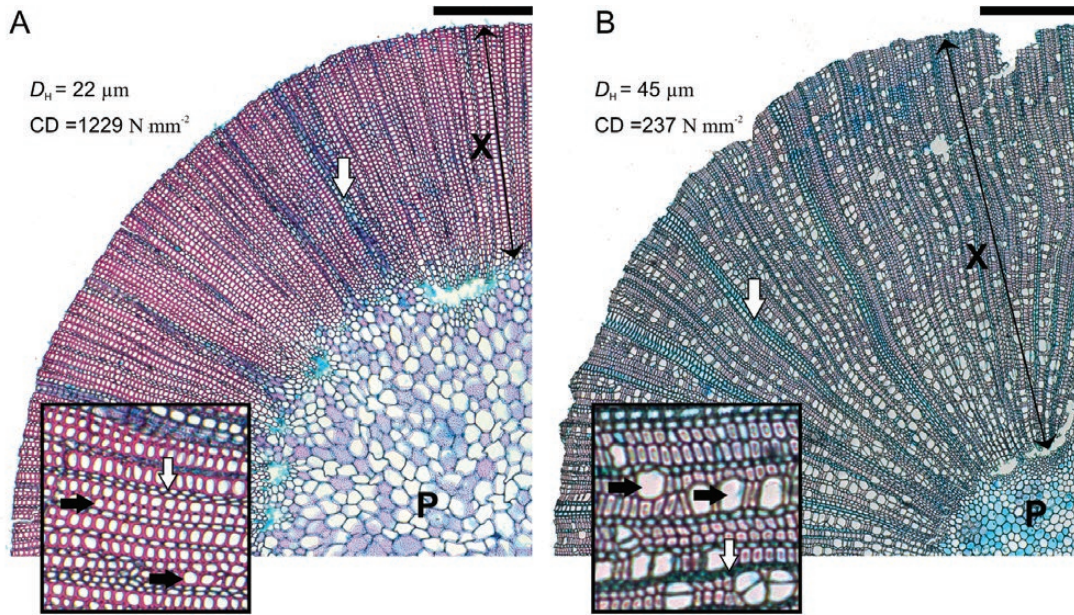


Fig. 1. Transverse microscopic wood sections of the vesselless *Amborella trichopoda* (a) and the vessel-bearing *Ascarina rubricaulis* (b) observed with a light microscope. Black arrows indicate tracheids (a) or vessels (b). Compelling differences in xylem conduit diameter (D_H) and conduit density (CD) are observed. Both species present uniseriate and multiseriate rays (white arrows). P=pith; X=xylem. Scale bars=500 μm , and 225 μm for insets.

Table 3. Differences in anatomical and hydraulic trait values between vesselless angiosperms ($n=5$) and vessel-bearing species with scalariform perforation plates ($n=7$)

Trait	Mean vesselless	Mean vessel-bearing	t	df	P
CD	1092	202	12.57	4.94	<0.001
D_H	22.60	38.45	-7.17	8.55	<0.001
D_m	8.81	9.07	-0.25	9.51	0.8061
D_{pa}	1.74	3.01	-1.93	6.54	0.0973
K_s	0.52	0.37	1.10	8.52	0.2998
K_{th}	7.26	12.58	-1.58	7.89	0.1527
L_p	1084	980	0.98	8.92	0.3545
P_{12}	-2.30	-1.46	2.21	6.60	0.0652
P_{50}	-2.85	-2.55	0.81	6.10	0.4478
S_{50}	102	45	3.27	5.47	<0.05
T_w	10.36	7.03	2.13	4.81	0.0880
T_m	258	266	-0.26	7.74	0.8041
$(t/b)^2$	0.338	0.049	3.52	4.03	<0.05

Mean trait values for each vascular type, list of statistics (t), degrees of freedom (df), and significance values (P) of independent t -tests are provided. Graphical comparisons of focal traits are provided in Fig. 2. Significant correlations are shown in bold. See Table 1 for a list of abbreviations and units.

of -2.85 ± 0.32 MPa, and vessel-bearing species showed a similar mean P_{50} of -2.55 ± 0.17 MPa (Fig. 2f; Table 3). Average P_{50} ranged from -4.11 MPa in the tracheid-bearing *Z. crassifolium* to -2.02 MPa in the vessel-bearing *P. alticola*, the most vulnerable species to drought-induced xylem embolism in our data set (Fig. 4). P_{12} was also not significantly different between conduit types: vesselless species had a mean P_{12} of -2.30 ± 0.55 MPa, and vessel-bearing species had a mean P_{12} of -1.46 ± 0.73 MPa (Table 3). Average P_{12} ranged from -3.50 MPa in the tracheid-bearing *Z. crassifolium* to -0.77 MPa in the vessel-bearing *P. alticola*. Interestingly, regardless of the xylem embolism index considered, these species were the most and the least resistant species, respectively (Table 2). P_{50} and P_{12} were not significantly

related to hydraulic efficiency, as expressed by K_{th} and K_s (Table 4). S_{50} varied from 24% in *H. cupulata* to a steep slope of 162% in *Z. acsmithii*. Vesselless species had a significantly steeper slope than vessel-bearing species (Fig. 2e; Table 3).

Relationships between xylem hydraulics and anatomical traits

Among the anatomical variables measured in this study, only T_m was significantly related to significant vulnerability to drought-induced embolism, as represented by P_{50} (Fig. 5a; Table 4): species with thicker pit membranes were less vulnerable to xylem embolism (Fig. 6). The relationship between T_m

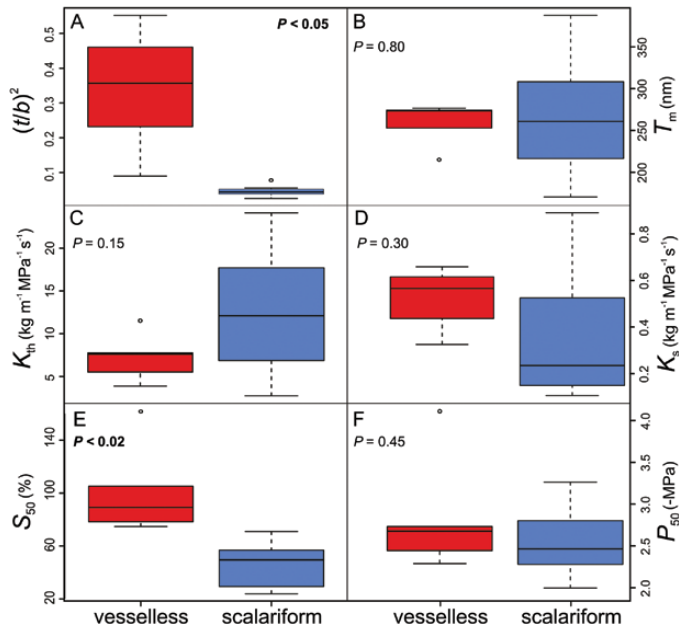


Fig. 2. Comparison of hydraulic and anatomical trait values amongst vesselless (red boxes) and vessel-bearing species with scalariform perforation plates (blue boxes). Boxes and bars show the median, 0.25 and 0.75 percentiles, and extreme values. P -values of comparisons between species with different xylem conduit types are included.

and P_{50} was highly significant when considering only vessel-bearing species (Fig. 5a), but not significant when considering only vesselless species (Fig. 5a) mainly because of the effect of *Z. crassifolium*, an outlier which had relatively thin interconduit pit membranes with respect to its high embolism resistance. We did not observe a significant relationship between T_m and P_{12} , the second index of embolism vulnerability included in this study (Table 4). Other ultrastructural pit features such as D_{pa} , D_m , and L_p were not related to P_{50} (Fig. 5b; Table 4). However, P_{12} was correlated with anatomical features such as CD, $(t/b)^2$, L_p , and T_w (Table 4). Multiple regression analyses including the joint effect of L_p and T_m on xylem embolism vulnerability showed a non-significant variation of P_{12} and P_{50} (Supplementary Table S1). The coefficients associated with L_p or T_m were not significant in both models (Supplementary Table S1). However, L_p was the variable that contributed the most to P_{12} variation, and T_m was the variable that contributed the most to P_{50} variation, as shown by the higher semi-partial correlation values (Supplementary Table S1). The lower association of P_{50} with L_p was readily observed using ordinary least square regressions (Fig. 5b).

Furthermore, we observed a significant relationship of S_{50} and $(t/b)^2$ with CD, and a positive correlation of D_{pa} and D_H with K_{th} . We found less significant intertrait correlations after phylogenetic corrections (Table 4). This might result from a more limited correlated evolution between traits, and because of the lower number of species considered in the analysis. Significant Pearson and PIC correlations were observed between anatomical features such as L_p and T_w . Moreover, the relationships of CD with S_{50} , and of D_H with K_{th} remained significant after phylogenetic correction. A complete list of coefficients of Pearson (r) and phylogenetic independent contrast

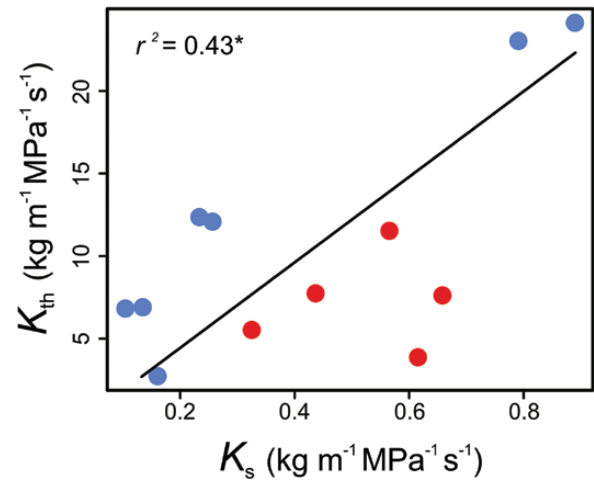


Fig. 3. Relationship between theoretical hydraulic conductivity based on anatomical measurements (K_{th}) and measured stem-specific hydraulic conductivity (K_s). Vessel-bearing species (blue points) and vesselless species (red points) are indicated. SMA regression is included. $*P < 0.05$.

correlations (r_{PIC}) between hydraulic and anatomical traits across species is available in Table 4.

Discussion

Similar hydraulic efficiency and safety in stems of vesselless and vessel-bearing angiosperms with scalariform perforation plates

Vesselless and vessel-bearing angiosperm species with scalariform perforation plates had similar hydraulic performance when considering both measured (K_s) and theoretical (K_{th}) xylem-specific hydraulic conductivity (Fig. 2; Table 3), confirming previous observations at the sapwood level (Hacke *et al.*, 2007; Sperry *et al.*, 2007; Hudson *et al.*, 2010). Based on the tight relationship between K_{th} and K_s , we obtained a satisfactory prediction of stem hydraulic conductivity using xylem anatomical measurements regardless of the xylem conduit type. The higher rates of K_{th} , as compared with K_s , arise from the underestimation of a number of structural features that can exert additional resistance to flow, such as perforation plate morphology and ultrastructural interconduit pit variation (Sperry *et al.*, 2007; Christman and Sperry, 2010; Hacke *et al.*, 2017). For instance, single-vessel flow measurements have demonstrated that scalariform perforation plates contribute significantly to the resistance to water flow, presenting 580% higher resistance at the sapwood level compared with species with vessels bearing simple perforation plates (Christman and Sperry, 2010). Moreover, interconduit pits account for >50% of total xylem hydraulic resistance in angiosperms (Sperry *et al.*, 2006; Choat *et al.*, 2008), mainly caused by the thickness of the pit membranes and the diameters of the pit apertures, emphasizing the strong influence of pit-level ultrastructural differences on hydraulic conductivity.

Only two vessel-bearing species, *A. rubricaulis* and *N. viellardii*, had higher K_s values than the vesselless species studied. Interestingly, *A. rubricaulis* and *N. viellardii* were the studied

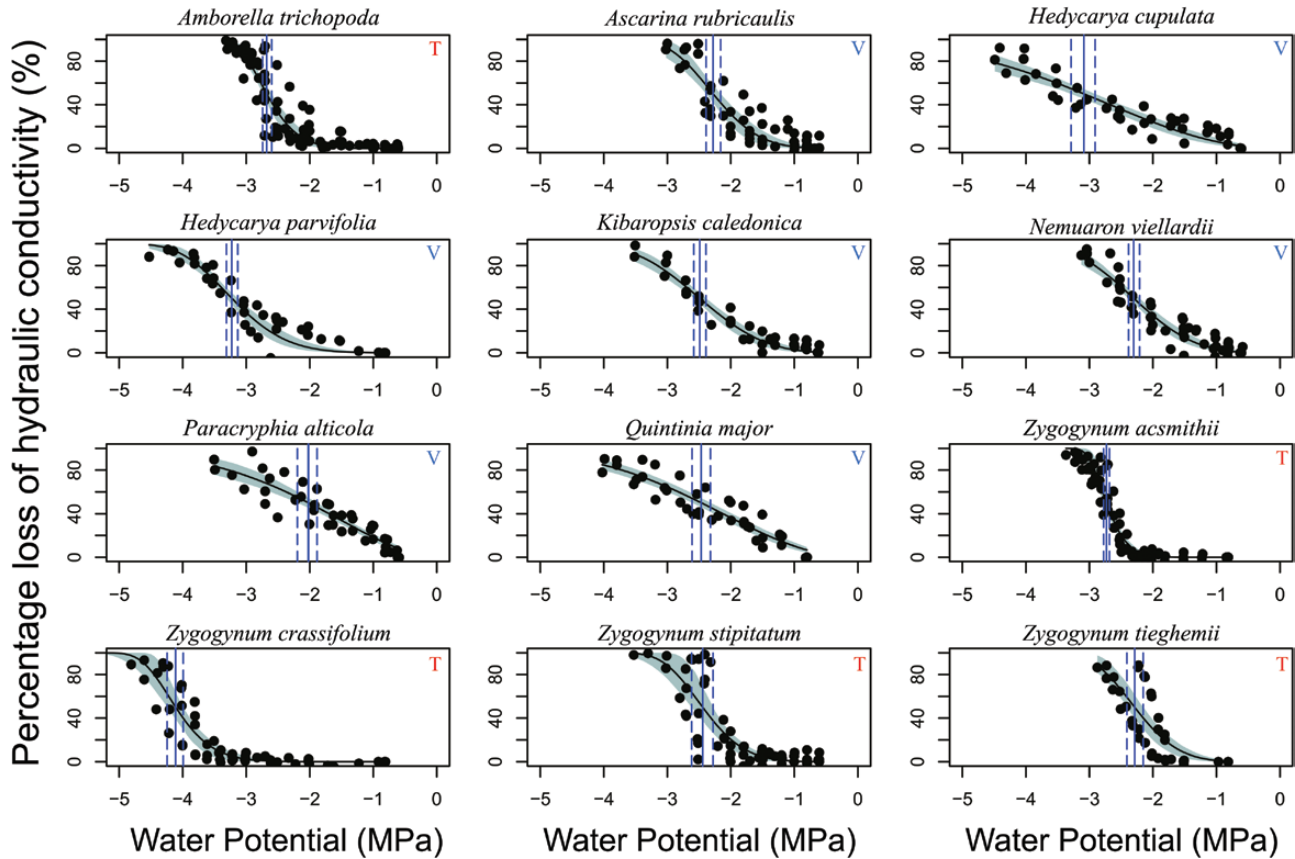


Fig. 4. Vulnerability curves fitted using a Weibull model showing the percentage loss of xylem hydraulic conductivity (%) as a function of declining water potential (MPa) for each of the 12 species studied. The best fit line is provided, and shaded polygons represent 95% confidence intervals (CIs). Vertical blue lines indicate the xylem pressure inducing 50% loss of hydraulic conductivity (P_{50}) including the 95% CI (dashed lines). Vesselless species bearing only tracheids (T) and vessel-bearing species with scalariform perforation plates (V) are indicated.

Table 4. Pearson and phylogenetic independent contrast correlations between hydraulic and anatomic traits

	P_{12}	P_{50}	S_{50}	K_s	K_{th}	$(t/b)^2$	CD	D_H	T_w	T_m	L_p	D_{pa}	D_m
P_{12}		0.84***	0.64*	0.32	-0.11	0.60*	0.61*	-0.42	0.58*	0.41	0.65*	-0.25	0.30
P_{50}	0.89**		0.20	-0.05	-0.28	0.43	0.25	-0.25	0.40	0.58*	0.54	-0.26	0.24
S_{50}	0.23	0.09		0.48	0.07	0.42	0.83***	-0.50	0.39	0	0.31	-0.22	0.03
K_s	0.19	0.11	0		0.65*	0.31	0.32	0.23	0.34	-0.18	0.46	0.44	0.19
K_{th}	0.12	0.53	0.78*	0.29		-0.42	-0.30	0.72**	-0.23	0.01	0.19	0.67*	0.09
$(t/b)^2$	0.34	0.50	0.74	0.44	0.71		0.69*	-0.76**	0.9***	-0.06	0.50	-0.33	0.13
CD	0.31	0.16	0.78*	0.02	0.34	0.37		-0.85***	0.48	-0.11	0.20	-0.44	-0.14
D_H	0.07	0.40	0.44	0.23	0.81*	0.51	0.19		-0.48	0.23	0	0.63*	0.16
T_w	0.36	0.20	0.35	0.83*	0.05	0.70	0.41	0.22		0.11	0.70*	-0.22	0.23
T_m	0.34	0.37	0.11	0.02	0.08	0.19	0.31	0.36	0.4		0.65*	0.01	0.29
L_p	0.39	0.28	0.34	0.67	0.06	0.63	0.47	0.31	0.94**	0.67		0.19	0.50
D_{pa}	0.25	0.07	0.76*	0.13	0.39	0.49	0.86*	0.13	0.52	0.61	0.65		0.39
D_m	0.73	0.54	0.07	0.51	0.01	0.47	0.27	0.32	0.80*	0.51	0.81*	0.27	

Correlations based on average values of vesselless and vessel-bearing angiosperm species. Pearson correlation coefficients (r) and phylogenetic independent contrast correlations (PICs) values are provided above and below the diagonal, respectively. PIC analyses were performed on a subset of nine species (see the Materials and methods). Significant correlations are shown in bold. * $P \leq 0.05$; ** $P \leq 0.01$; *** $P \leq 0.001$. See Table 1 for abbreviations and units.

species with the highest average D_H measured, illustrating the relevance of conduit diameter in increasing hydraulic conductivity. The low K_s values measured in the remaining vessel-bearing species probably result from the morphology of their

perforation plates, since they all present oblique scalariform perforation plates with numerous, closely spaced bars (often >20 ; Fig. 7a, b). *Paracryphia alticola*, one of the species with the lowest K_s measured (Table 2), is noteworthy in this regard because of

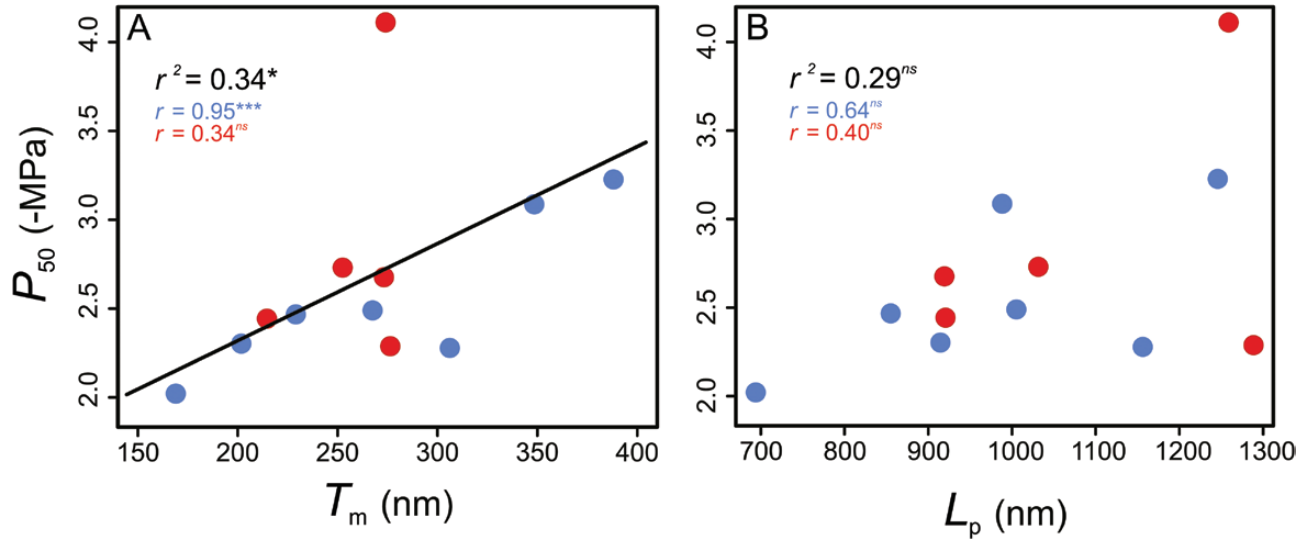


Fig. 5. Relationship of pit ultrastructural traits to xylem embolism vulnerability. (A) The thickness of the interconduit pit membrane (T_m) is significantly related to xylem embolism vulnerability (P_{50}). (B) Lack of a relationship between depth of pit chamber (L_p) and embolism vulnerability (P_{50}). Vessel-bearing species with scalariform perforation plates (blue points) and vesselless species (red points) along with correlation values for each vascular type are indicated. *ns*=non significant; * $P \leq 0.05$; *** $P \leq 0.001$.

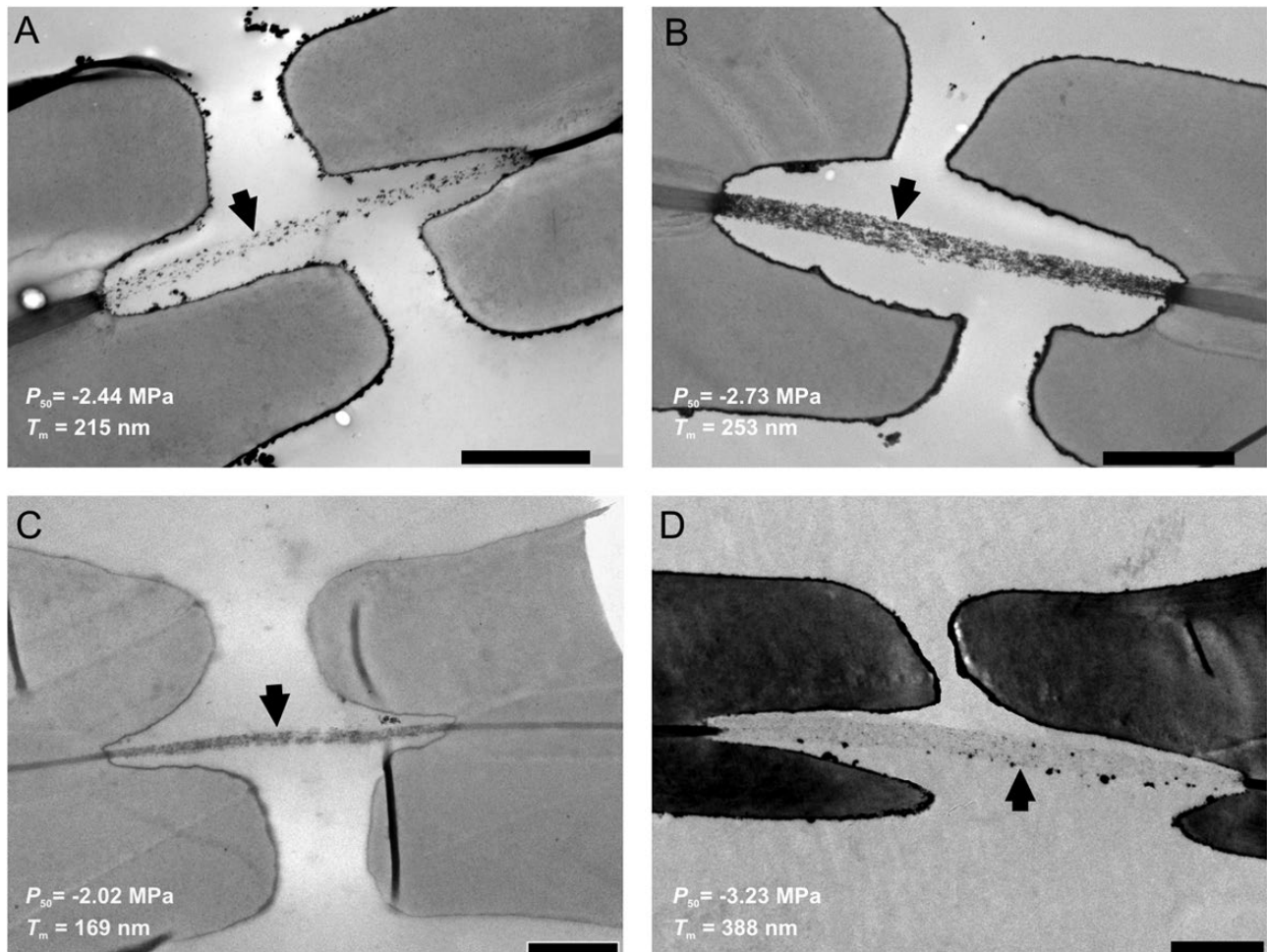


Fig. 6. TEM images of interconduit lateral pits in vesselless (A, B) and vessel-bearing (C, D) angiosperms illustrating species that are vulnerable to embolism (left) and more embolism-resistant species (right). (A) *Zygogynum stipitatum*. (B) *Zygogynum acsmithii*. (C) *Paracryphia alticola*. (D) *Hedycarya parvifolia*. Arrows indicate pit membranes. Scale bars=2 μm .

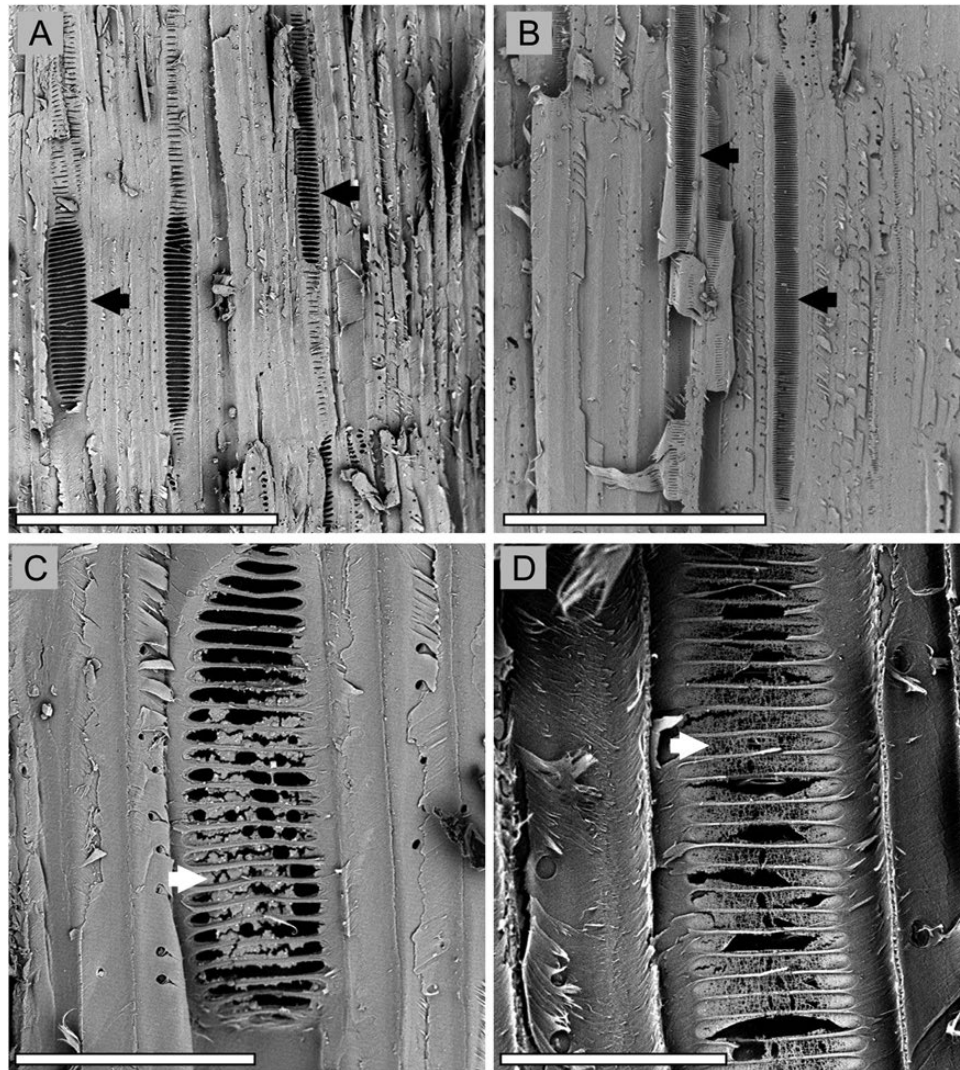


Fig. 7. SEM images of vessel elements bearing scalariform perforation plates with different morphologies. (a and b) Radial view of scalariform perforation plates (black arrows). (c and d) Membrane remnants in pits of scalariform perforation plates (white arrows). (a, c) *Hedycarya cupulata*. (b, d) *Paracryphia alticola*. Scale bars=150 μm in (a) and (b); 70 μm in (c); 30 μm in (d).

the exceptionally high number of bars per perforation plate (on average >100 , with maximum values of up to 200 according to Dickison and Baas, 1977; Fig. 7b). The observed similarities in hydraulic efficiency across vesselless and vessel-bearing angiosperms with scalariform perforation plates underpin the view that efficient vessel-bearing species emerged only after the reduction of bars in the scalariform perforation plates and the development of highly efficient simple perforation plates in which all the bars have disappeared. It has been shown that the tracheids of vesselless angiosperms have a lower pit area resistivity in comparison with those of eudicot vessels (Hacke et al., 2007). However, Sperry et al. (2007) estimated that the more efficient eudicot angiosperms, which are over-represented by species with simple perforation plates, have ~ 4.5 times lower sapwood-specific resistivity than early diverging angiosperms, including both vessel-bearing and vesselless lineages.

Along with perforation plate morphology, it has been suggested that pit membrane remnants further increase sap flow resistivity (Carlquist, 1992; Sperry et al., 2007; Feild and Wilson, 2012). Pit membrane remnants, observed in the scalariform

perforation plates of the species studied here (Fig. 7c, d), are considered to be a relictual character in angiosperms and are regularly observed in angiosperm species with densely barred scalariform perforation plates (Carlquist, 1992; Carlquist and Schneider, 2004). Incomplete lysis of the cellulose microfibrils in developing scalariform perforation plates causes this transitional stage between tracheids (with intact pit membranes in scalariform end wall pitting) and vessel elements (with none or residual pit membrane remnants in the scalariform perforation plates; Carlquist, 1992). Taken all together, scalariform perforation plates with many bars and pit membrane remnants represent major obstructions to flow, accounting for 57% of the total flow resistivity on average (Sperry et al., 2007).

In addition to the comparable hydraulic efficiency between the vesselless and vessel-bearing angiosperm species studied, our observations also showed no differences in vulnerability to xylem embolism (P_{12} and P_{50}) between both groups. The similar low efficiency and safety in xylem hydraulic transport observed here in both groups supports the hypothesis that early diverging angiosperms were limited to mesic habitats with low

evaporative demands and low drought-induced embolism resistance throughout their evolutionary history (Sperry *et al.*, 2007; Carlquist, 2012; Feild and Wilson, 2012). On the other hand, species with different conduit types showed significant differences in S_{50} obtained from vulnerability curves fitted using a Weibull function, suggesting that the drought-induced loss in hydraulic conductivity occurs faster in vesselless species. This difference in speed of hydraulic dysfunction between vessel-bearing and vesselless species may be caused by the higher conduit density of vesselless species, and thus more numerous pit connections between tracheids that enable air to propagate faster within the 3D tracheid network. We did not find a clear safety–efficiency trade-off in our data set, which is in line with the weak relationship between xylem hydraulic safety and efficiency observed in woody species across different ecosystems (Gleason *et al.*, 2016a).

Anatomical features conferring embolism resistance in angiosperms with different xylem conduit morphologies: the key role of interconduit pit membrane thickness

Our study highlights that pit structural traits are the most important anatomical feature in determining xylem embolism resistance. Indeed, among all measured xylem conduit features, interconduit pit membrane thickness (T_m) was the only trait that was significantly linked to significant levels of embolism resistance (P_{50}). Overall, species with thicker interconduit pit membranes showed higher resistance to drought-induced embolism formation, which is in agreement with previous studies across a diversity of angiosperm species (Lens *et al.*, 2011; Li *et al.*, 2016; Dória *et al.*, 2018, 2019). Due to the accumulation of cellulose microfibril layers in the interconduit pit membranes, species with thicker pit membranes have a longer and more tortuous pathway for air bubbles to traverse from an embolized conduit to an adjacent water-filled conduit. Moreover, it is believed that thicker interconduit pit membranes have more lipid-based surfactant molecules in the intervessel pit membranes, which may facilitate coating of the nanoscaled air bubbles, thereby stabilizing these nanobubbles under negative pressure (Schenk *et al.*, 2015, 2017). Additionally, higher T_m might allow for safeguarding the mechanical integrity at high cavitation-inducing tensions (Tixier *et al.*, 2014), thereby preventing the pores in the pit membranes from enlarging above a critical air-seeding threshold.

The relationship between T_m and P_{50} was not significant when considering vesselless species only. The lack of T_m – P_{50} correlation observed in the vesselless angiosperms studied might stem from a low variation in embolism vulnerability thresholds. However, our results—matching anatomical and hydraulic observations from the same stems—are consistent with a recent study that could not detect a functional T_m – P_{50} correlation in six vesselless angiosperm species based on anatomical and hydraulic observations that came from different individuals (Zhang *et al.*, 2017; Supplementary Table S2). When merging our data with the data set of Zhang *et al.* (2017), we were still unable to detect a significant correlation between T_m and P_{50} amongst the vesselless species ($r = -0.27$; $P = 0.45$;

Supplementary Fig. S2). Future studies with a denser sampling, combining hydraulic and anatomical measurements from the same individuals, are necessary to explore further the relationship between T_m and P_{50} in vesselless angiosperm species. The lack of PIC correlations observed between T_m and P_{50} suggests that the evolutionary basis for a coordination between pit membrane thickness and increased embolism resistance is weak. However, this analysis was performed on only nine out of the 12 species measured due to incomplete sampling in published molecular phylogenies. Future studies including phylogenetic corrections would be needed to understand the evolutionary significance of xylem conduit ultrastructural variation, and its link to embolism resistance in the plant hydraulic system.

Conduit diameter was not related to drought-induced embolism vulnerability in our study. This is in accordance with Tyree and Sperry (1989) who argued that the mechanism of embolism formation is not directly linked to conduit diameter. The relationship between drought-inducing embolism and D_H is controversial: large trees tend to be more prone to drought-induced mortality compared with shorter trees (Bennett *et al.*, 2015) probably because plant size is the main driver of conduit diameter variation (Olson *et al.*, 2018), but sound evidence for this correlation at the high (Hacke *et al.*, 2017) or low taxonomic level (Fichot *et al.*, 2010; Lens *et al.*, 2011) is ambiguous. Our results in branches of comparable diameter and position in the crown suggest that conduit diameter and embolism vulnerability are unrelated across angiosperms with different conduit morphologies. Likewise, we did not find a significant relationship between CD and P_{50} , and species with different types of tracheary elements showed similar embolism-inducing pressure thresholds. Nevertheless, CD was significantly correlated to S_{50} across species, and this relationship was also significant using PIC correlation analyses. The relationship between CD and S_{50} suggests that tracheid-bearing species with numerous adjacent conduits per xylem surface area have a faster propagation of embolisms via air-seeding compared with vessel-bearing species with fewer conduits. P_{12} , which has been suggested as an air-entry threshold (Domec and Gartner, 2001; Martin-StPaul *et al.*, 2017), was correlated to CD, L_p , T_w , and $(t/b)^2$. Moreover, the pit chamber depth (L_p) showed a higher semi-partial correlation value than pit membrane thickness (T_m) when explaining the joint effect of both structural features on P_{12} . These results suggest an important role for conduit wall features and pit chamber depth on air propagation under low xylem tensions.

One of the features that diverged between vesselless and vessel-bearing species was cell wall reinforcement or the thickness to span ratio of conduits, as represented by $(t/b)^2$. A similar index, $(t/b)^3$, has been shown to be significantly related to climate variables and leaf P_{50} in Australian angiosperms (Blackman *et al.*, 2010; Jordan *et al.*, 2013). Yet, conduit wall reinforcement was unrelated to embolism vulnerability in our set of species: vesselless species presented significantly higher $(t/b)^2$ than vessel-bearing species, but both groups showed similar embolism vulnerability values. Therefore, it seems that conduit wall reinforcement is not selected for in moist rain forest habitats, as opposed to the strong relationship of $(t/b)^2$

and P_{50} in drier vegetation types such as southern Californian chaparral (Jacobsen *et al.*, 2005). Additionally, tracheids are simultaneously involved in the mechanical and hydraulic functions of vesselless angiosperms (Hudson *et al.*, 2010; Feild and Wilson, 2012; Feild *et al.*, 2012). Therefore, the higher conduit wall reinforcement in vesselless angiosperms might be selected to meet the mechanical demands of the stems, blurring the relationship between $(t/b)^2$ and P_{50} . $(t/b)^2$ was, however, related to P_{12} , suggesting an important role for conduit wall reinforcement during the onset of xylem embolism formation.

New Caledonian rain forests, a safe haven for species with inefficient and drought-sensitive xylem conduits

It has been suggested that the high hydraulic resistance exerted by oblique scalariform perforation plates may not be disadvantageous in environments with low transpiration rates such as tropical mountains and cool alpine regions (Baas, 1976; Carlquist, 2001; Jansen *et al.*, 2004; Lens *et al.*, 2016). Likewise, vesselless angiosperms might be limited to wet forest habitats where their tracheid-based wood does not impose important hydraulic constraints, and may also be favored in freezing-prone environments (Feild *et al.*, 2000, 2002). Given that the species included in this study are mainly distributed in rain forest ecosystems (Trueba *et al.*, 2017), our results suggest that the species studied, which are characterized by low hydraulic safety and efficiency, have not experienced past climatic conditions that forced them to evolve a hydraulically efficient and embolism-resistant vascular apparatus. Species with both low efficiency and low safety are more common than expected (Gleason *et al.*, 2016a), and the occurrence of species with this hydraulic profile in the New Caledonian archipelago might be explained by the presence of rain forest refugia during the climatic upheavals of the Pleistocene (Pouteau *et al.*, 2015). Likewise, the persistence of mesic climatic conditions may have buffered New Caledonian species with vulnerable xylem conduits from the extreme climate shifts that strongly affected the vegetation of Australia and some nearby South Pacific Islands (Byrne *et al.*, 2011).

Most of the species studied here are considered early diverging angiosperms because of their phylogenetic position, belonging to the ANA grade and the magnoliids, with the massive monocot–eudicot clade as a subsequently diverging clade. New Caledonian early diverging angiosperms have a remarkable preference for rain forest habitats that exhibit high moisture levels and low diurnal and seasonal variations in temperature (Pouteau *et al.*, 2015). Xylem embolism and its associated hydraulic failure is one of the most important mechanisms driving drought-induced mortality in moist tropical forests (Adams *et al.*, 2017; McDowell *et al.*, 2018). It has been shown that species inhabiting similar environments can display different drought tolerances, ultimately showing different mortality rates after a drought event (Johnson *et al.*, 2018). However, the lack of differentiation in hydraulic vulnerability between vessel-bearing angiosperms with scalariform perforation plates and co-occurring vesselless species suggests that, under the stable climatic conditions of the New Caledonian

rain forest, species with different conduit types show a convergence of wood physiological features (Brodribb and Feild, 2000). Given ongoing and projected increases in temperature averages in New Caledonia (Cavarero *et al.*, 2012), our results suggest that drought will equally impact species with xylem conduits displaying very different morphologies. Extreme climate events in the rain forests of New Caledonia may therefore represent a major threat to the unique and charismatic flora of the archipelago.

Supplementary data

Supplementary data are available at JXB online.

Fig. S1. Phylogenetic tree showing the relationships of nine of the 12 studied species.

Fig. S2. Relationship of embolism vulnerability (P_{50}) and pit membrane thickness (T_m) across vesselless angiosperms.

Table S1. Multiple regressions showing embolism vulnerability (P_{12} and P_{50}) as predicted by the joint effect of ultrastructural variables: pit membrane thickness (T_m) and pith chamber depth (L_p).

Table S2. Hydraulic vulnerability (P_{50}) and pit membrane thickness (T_m) of 10 vesselless angiosperms.

Acknowledgements

We thank Jeremy Girardi for assistance during fieldwork and light microscope image processing, Vanessa Hequet for fieldwork assistance, Fabian Carriconde, Valérie Medevielle, and Léocadie Jamet for providing laboratory equipment, Rob Langelaan for assistance in the preparation of samples and TEM imaging, Felipe Zapata and Leila Fletcher for providing help in the implementation of PIC analysis, and Tim Brodribb, Taylor Feild, and Adam Roddy for their insightful comments on the manuscript. ST was supported by CONACYT (grant no. 217745) and by the UC-MEXUS postdoctoral program. This work was also supported by the ‘Investments for the Future’ (ANR-10-EQPX-16, XYLOFOREST) program and the Cluster of Excellence COTE (ANR-10-LABX-45, within the DEFI project) of the French National Agency for Research.

References

- Adams HD, Zeppel MJ, Anderegg WR, *et al.* 2017. A multi-species synthesis of physiological mechanisms in drought-induced tree mortality. *Nature Ecology & Evolution* **1**, 1285.
- Baas P. 1976. Some functional and adaptive aspects of vessel member morphology. In: Baas P, Bolton AJ, Catling DM, eds. *Wood structure in biological and technological research*. Leiden, The Netherlands: Leiden University Press, 157–181.
- Badel E, Ewers FW, Cochard H, Telewski FW. 2015. Acclimation of mechanical and hydraulic functions in trees: impact of the thigmomorphogenetic process. *Frontiers in Plant Science* **6**, 266.
- Bailey IW. 1944. The development of vessels in angiosperms and its significance in morphological research. *American Journal of Botany* **31**, 421–428.
- Bailey IW, Tupper WW. 1918. Size variation in tracheary cells: I. A comparison between the secondary xylems of vascular cryptogams, gymnosperms and angiosperms. *Proceedings of the American Academy of Arts and Sciences, USA* **54**, 149–204.
- Bennett AC, McDowell NG, Allen CD, Anderson-Teixeira KJ. 2015. Larger trees suffer most during drought in forests worldwide. *Nature Plants* **1**, 15139.

- Blackman CJ, Brodribb TJ, Jordan GJ.** 2010. Leaf hydraulic vulnerability is related to conduit dimensions and drought resistance across a diverse range of woody angiosperms. *New Phytologist* **188**, 1113–1123.
- Bouche PS, Larter M, Domec JC, Burtlett R, Gasson P, Jansen S, Delzon S.** 2014. A broad survey of hydraulic and mechanical safety in the xylem of conifers. *Journal of Experimental Botany* **65**, 4419–4431.
- Brodersen C, Jansen S, Choat B, Rico C, Pittermann J.** 2014. Cavitation resistance in seedless vascular plants: the structure and function of interconduit pit membranes. *Plant Physiology* **165**, 895–904.
- Brodribb TJ, Feild TS.** 2000. Stem hydraulic supply is linked to leaf photosynthetic capacity: evidence from New Caledonian and Tasmanian rainforests. *Plant, Cell & Environment* **23**, 1381–1388.
- Brodribb TJ, Feild TS.** 2010. Leaf hydraulic evolution led a surge in leaf photosynthetic capacity during early angiosperm diversification. *Ecology Letters* **13**, 175–183.
- Byrne M, Steane DA, Joseph L, et al.** 2011. Decline of a biome: evolution, contraction, fragmentation, extinction and invasion of the Australian mesic zone biota. *Journal of Biogeography* **38**, 1635–1656.
- Carlquist S.** 1992. Pit membrane remnants in perforation plates of primitive dicotyledons and their significance. *American Journal of Botany* **79**, 660–672.
- Carlquist S.** 2001. *Comparative wood anatomy*. Berlin Heidelberg: Springer.
- Carlquist S.** 2012. How wood evolves: a new synthesis. *Botany* **90**, 901–940.
- Carlquist S, Schneider EL.** 2002a. The tracheid–vessel element transition in angiosperms involves multiple independent features: cladistic consequences. *American Journal of Botany* **89**, 185–195.
- Carlquist S, Schneider EL.** 2002b. Vessels of Illicium (Illiciaceae): range of pit membrane remnant presence in perforations and other vessel details. *International Journal of Plant Sciences* **163**, 755–763.
- Carlquist S, Schneider EK.** 2004. Perforation plate pit membrane remnants and other vessel details of clethraceae: primitive features in wood of Ericales. *International Journal of Plant Sciences* **165**, 369–375.
- Cavarero V, Peltier A, Aubail X, et al.** 2012. Les évolutions passées et futures du climat de la Nouvelle-Calédonie. *La Météorologie* **77**, 13–21.
- Choat B, Cobb AR, Jansen S.** 2008. Structure and function of bordered pits: new discoveries and impacts on whole-plant hydraulic function. *New Phytologist* **177**, 608–626.
- Choat B, Jansen S, Brodribb TJ, et al.** 2012. Global convergence in the vulnerability of forests to drought. *Nature* **491**, 752–755.
- Christman MA, Sperry JS.** 2010. Single-vessel flow measurements indicate scalariform perforation plates confer higher flow resistance than previously estimated. *Plant, Cell & Environment* **33**, 431–443.
- Cochard H, Damour G, Bodet C, Tharwat I, Poirier M, Améglio T.** 2005. Evaluation of a new centrifuge technique for rapid generation of xylem vulnerability curves. *Physiologia Plantarum* **124**, 410–418.
- Delzon S, Douthe C, Sala A, Cochard H.** 2010. Mechanism of water-stress induced cavitation in conifers: bordered pit structure and function support the hypothesis of seal capillary-seeding. *Plant, Cell & Environment* **33**, 2101–2111.
- Dickison WC, Baas P.** 1977. The morphology and relationships of Paracryphia (Paracryphiaceae). *Blumea* **23**, 417–438.
- Domec J-C, Gartner BL.** 2001. Cavitation and water storage capacity in bole xylem segments of mature and young Douglas-fir trees. *Trees* **15**, 204–214.
- Dória LC, Meijs C, Podadera DS, Del Arco M, Smets E, Delzon S, Lens F.** 2019. Embolism resistance in stems of herbaceous Brassicaceae and Asteraceae is linked to differences in woodiness and precipitation. *Annals of Botany* (in press).
- Dória LC, Podadera DS, Arco M, Chauvin T, Smets E, Delzon S, Lens F.** 2018. Insular woody daisies (Argyranthemum, Asteraceae) are more resistant to drought-induced hydraulic failure than their herbaceous relatives. *Functional Ecology* **32**, 1467–1478.
- Duursma R, Choat B.** 2017. fitplc: an R package to fit hydraulic vulnerability curves. *Journal of Plant Hydraulics* **4**, e002.
- Feild TS, Arens NC.** 2007. The ecophysiology of early angiosperms. *Plant, Cell & Environment* **30**, 291–309.
- Feild TS, Arens NC, Dawson TE.** 2003. The ancestral ecology of angiosperms: emerging perspectives from extant basal lineages. *International Journal of Plant Sciences* **164**, S129–S142.
- Feild TS, Arens NC, Doyle JA, Dawson TE, Donoghue MJ.** 2004. Dark and disturbed: a new image of early angiosperm ecology. *Paleobiology* **30**, 82–107.
- Feild TS, Brodribb TJ.** 2013. Hydraulic tuning of vein cell microstructure in the evolution of angiosperm venation networks. *New Phytologist* **199**, 720–726.
- Feild TS, Brodribb T, Holbrook NM.** 2002. Hardly a relict: freezing and the evolution of vesselless wood in Winteraceae. *Evolution* **56**, 464–478.
- Feild TS, Chatelet DS, Balun L, Schilling EE, Evans R.** 2012. The evolution of angiosperm lianescent without vessels—climbing mode and wood structure–function in *Tasmania cordata* (Winteraceae). *New Phytologist* **193**, 229–240.
- Feild TS, Hudson PJ, Balun L, Chatelet DS, Patino AA, Sharma CA, McLaren K.** 2011. The ecophysiology of xylem hydraulic constraints by ‘basal’ vessels in *Canella winterana* (Canellaceae). *International Journal of Plant Sciences* **172**, 879–888.
- Feild TS, Wilson JP.** 2012. Evolutionary voyage of angiosperm vessel structure–function and its significance for early angiosperm success. *International Journal of Plant Sciences* **173**, 596–609.
- Feild TS, Zwieniecki MA, Holbrook NM.** 2000. Winteraceae evolution: an ecophysiological perspective. *Annals of the Missouri Botanical Garden* **87**, 323–334.
- Felsenstein J.** 1985. Phylogenies and the comparative method. *The American Naturalist* **125**, 1–15.
- Fichot R, Barigah TS, Chamillard S, LE Thiec D, Laurans F, Cochard H, Brignolas F.** 2010. Common trade-offs between xylem resistance to cavitation and other physiological traits do not hold among unrelated *Populus deltoides* × *Populus nigra* hybrids. *Plant, Cell & Environment* **33**, 1553–1568.
- Gleason SM, Westoby M, Jansen S, et al.** 2016a. Weak tradeoff between xylem safety and xylem-specific hydraulic efficiency across the world’s woody plant species. *New Phytologist* **209**, 123–136.
- Gleason SM, Westoby M, Jansen S, et al.** 2016b. On research priorities to advance understanding of the safety–efficiency tradeoff in xylem. *New Phytologist* **211**, 1156–1158.
- Hacke UG, Sperry JS, Pockman WT, Davis SD, McCulloh KA.** 2001. Trends in wood density and structure are linked to prevention of xylem implosion by negative pressure. *Oecologia* **126**, 457–461.
- Hacke UG, Sperry JS, Feild TS, Sano Y, Sikkema EH, Pittermann J.** 2007. Water transport in vesselless angiosperms: conducting efficiency and cavitation safety. *International Journal of Plant Sciences* **168**, 1113–1126.
- Hacke UG, Sperry JS, Wheeler JK, Castro L.** 2006. Scaling of angiosperm xylem structure with safety and efficiency. *Tree Physiology* **26**, 689–701.
- Hacke UG, Spicer R, Schreiber SG, Plavcová L.** 2017. An ecophysiological and developmental perspective on variation in vessel diameter. *Plant, Cell & Environment* **40**, 831–845.
- Hudson PJ, Razanatsoa J, Feild TS.** 2010. Early vessel evolution and the diversification of wood function: insights from Malagasy Canellales. *American Journal of Botany* **97**, 80–93.
- Jacobsen AL, Ewers FW, Pratt RB, Paddock WA 3rd, Davis SD.** 2005. Do xylem fibers affect vessel cavitation resistance? *Plant Physiology* **139**, 546–556.
- Jansen S, Baas P, Gasson P, Lens F, Smets E.** 2004. Variation in xylem structure from tropics to tundra: evidence from vested pits. *Proceedings of the National Academy of Sciences, USA* **101**, 8833–8837.
- Jansen S, Choat B, Pletsers A.** 2009. Morphological variation of intervessel pit membranes and implications to xylem function in angiosperms. *American Journal of Botany* **96**, 409–419.
- Johnson DM, Domec J-C, Berry ZC, et al.** 2018. Co-occurring woody species have diverse hydraulic strategies and mortality rates during an extreme drought. *Plant, Cell & Environment* **41**, 576–588.
- Jordan GJ, Brodribb TJ, Blackman CJ, Weston PH.** 2013. Climate drives vein anatomy in Proteaceae. *American Journal of Botany* **100**, 1483–1493.

- Karnovsky MJ** 1965. A formaldehyde glutaraldehyde fixative of high osmolality for use in electron microscopy. *Journal of Cell Biology* **27**, 137–138.
- Lens F, Sperry JS, Christman MA, Choat B, Rabaey D, Jansen S.** 2011. Testing hypotheses that link wood anatomy to cavitation resistance and hydraulic conductivity in the genus *Acer*. *New Phytologist* **190**, 709–723.
- Lens F, Tixier A, Cochard H, Sperry JS, Jansen S, Herbette S.** 2013. Embolism resistance as a key mechanism to understand adaptive plant strategies. *Current Opinion in Plant Biology* **16**, 287–292.
- Lens F, Vos RA, Charrier G, et al.** 2016. Scalariform-to-simple transition in vessel perforation plates triggered by differences in climate during the evolution of Adoxaceae. *Annals of Botany* **118**, 1043–1056.
- Li S, Lens F, Espino S, Karimi Z, Klepsch M, Schenk HJ, Schmitt M, Schuldt B, Jansen S.** 2016. Intervessel pit membrane thickness as a key determinant of embolism resistance in angiosperm xylem. *Iawa Journal* **37**, 152–171.
- Loepfe L, Martinez-Vilalta J, Piñol J, Mencuccini M.** 2007. The relevance of xylem network structure for plant hydraulic efficiency and safety. *Journal of Theoretical Biology* **247**, 788–803.
- Magallón S, Gómez-Acevedo S, Sánchez-Reyes LL, Hernández-Hernández T.** 2015. A metacalibrated time-tree documents the early rise of flowering plant phylogenetic diversity. *New Phytologist* **207**, 437–453.
- Martin-StPaul N, Delzon S, Cochard H.** 2017. Plant resistance to drought depends on timely stomatal closure. *Ecology Letters* **20**, 1437–1447.
- McDowell N, Allen CD, Anderson-Teixeira K, et al.** 2018. Drivers and mechanisms of tree mortality in moist tropical forests. *New Phytologist* **219**, 851–869.
- Ogle K, Barber JJ, Willson C, Thompson B.** 2009. Hierarchical statistical modeling of xylem vulnerability to cavitation. *New Phytologist* **182**, 541–554.
- Olson ME.** 2014. Xylem hydraulic evolution, I. W. Bailey, and Nardini & Jansen (2013): pattern and process. *New Phytologist* **203**, 7–11.
- Olson ME, Soriano D, Rosell JA, et al.** 2018. Plant height and hydraulic vulnerability to drought and cold. *Proceedings of the National Academy of Sciences, USA* **115**, 7551–7556.
- Paradis E, Claude J, Strimmer K.** 2004. APE: analyses of phylogenetics and evolution in R language. *Bioinformatics* **20**, 289–290.
- Pittermann J, Choat B, Jansen S, Stuart SA, Lynn L, Dawson TE.** 2010. The relationships between xylem safety and hydraulic efficiency in the Cupressaceae: the evolution of pit membrane form and function. *Plant Physiology* **153**, 1919–1931.
- Pittermann J, Sperry J.** 2003. Tracheid diameter is the key trait determining the extent of freezing-induced embolism in conifers. *Tree Physiology* **23**, 907–914.
- Poorter L, McDonald I, Alarcón A, Fichtler E, Licona JC, Peña-Claros M, Sterck F, Villegas Z, Sass-Klaassen U.** 2010. The importance of wood traits and hydraulic conductance for the performance and life history strategies of 42 rainforest tree species. *New Phytologist* **185**, 481–492.
- Pouteau R, Trueba S, Feild TS, Isnard S.** 2015. New Caledonia: a Pleistocene refugium for rain forest lineages of relict angiosperms. *Journal of Biogeography* **42**: 2062–2077.
- R Core Team.** 2017. R: a language and environment for statistical computing. Vienna, Austria: R Foundation for Statistical Computing.
- Rosner S, Gierlinger N, Klepsch M, et al.** 2018. Hydraulic and mechanical dysfunction of Norway spruce sapwood due to extreme summer drought in Scandinavia. *Forest Ecology and Management* **409**, 527–540.
- Sano Y, Morris H, Shimada H, Ronse De Craene LP, Jansen S.** 2011. Anatomical features associated with water transport in imperforate tracheary elements of vessel-bearing angiosperms. *Annals of Botany* **107**, 953–964.
- Schenk HJ, Espino S, Romo DM, et al.** 2017. Xylem surfactants introduce a new element to the cohesion–tension theory. *Plant Physiology* **173**, 1177–1196.
- Schenk HJ, Steppe K, Jansen S.** 2015. Nanobubbles: a new paradigm for air-seeding in xylem. *Trends in Plant Science* **20**, 199–205.
- Scholz A, Klepsch M, Karimi Z, Jansen S.** 2013. How to quantify conduits in wood? *Frontiers in Plant Science* **4**, 56.
- Smith SA, Brown JW.** 2018. Constructing a broadly inclusive seed plant phylogeny. *American Journal of Botany* **105**, 302–314.
- Sperry JS.** 2003. Evolution of water transport and xylem structure. *International Journal of Plant Sciences* **164**, S115–S127.
- Sperry JS, Hacke UG, Feild TS, Sano Y, Sikkema EH.** 2007. Hydraulic consequences of vessel evolution in angiosperms. *International Journal of Plant Sciences* **168**, 1127–1139.
- Sperry JS, Hacke UG, Pittermann J.** 2006. Size and function in conifer tracheids and angiosperm vessels. *American Journal of Botany* **93**, 1490–1500.
- Spicer R, Groover A.** 2010. Evolution of development of vascular cambia and secondary growth. *New Phytologist* **186**, 577–592.
- Tixier A, Herbette S, Jansen S, Capron M, Tordjeman P, Cochard H, Badel E.** 2014. Modelling the mechanical behaviour of pit membranes in bordered pits with respect to cavitation resistance in angiosperms. *Annals of Botany* **114**, 325–334.
- Trueba S, Isnard S, Barthélémy D, Olson ME.** 2016. Trait coordination, mechanical behaviour and growth form plasticity of *Amborella trichopoda* under variation in canopy openness. *AoB Plants* **8**, plw068.
- Trueba S, Pouteau R, Lens F, Feild TS, Isnard S, Olson ME, Delzon S.** 2017. Vulnerability to xylem embolism as a major correlate of the environmental distribution of rain forest species on a tropical island. *Plant, Cell & Environment* **40**, 277–289.
- Tyree MT, Sperry JS.** 1989. Vulnerability of xylem to cavitation and embolism. *Annual Review of Plant Physiology and Plant Molecular Biology* **40**: 19–36.
- Tyree MT, Zimmermann MH.** 2002. Xylem structure and the ascent of sap. Berlin Heidelberg: Springer.
- Warton DI, Duursma RA, Falster DS, Taskinen S.** 2012. smatr 3—an R package for estimation and inference about allometric lines. *Methods in Ecology and Evolution* **3**, 257–259.
- Zanne AE, Westoby M, Falster DS, Ackerly DD, Loarie SR, Arnold SE, Coomes DA.** 2010. Angiosperm wood structure: global patterns in vessel anatomy and their relation to wood density and potential conductivity. *American Journal of Botany* **97**, 207–215.
- Zhang Y, Klepsch M, Jansen S.** 2017. Bordered pits in xylem of vesselless angiosperms and their possible misinterpretation as perforation plates. *Plant, Cell & Environment* **40**, 2133–2146.